Proceedings of the 29th Annual International
Conference of the IEEE EMBS
Cité Internationale, Lyon, France
August 23-26, 2007.

Stem-Cell Localization: A Deconvolution Problem

Nezamoddin N. Kachouie [1], Paul Fieguth [1], and Eric Jervis [2]
[1]Department of Systems Design Engineering
[2]Department of Chemical Engineeribg
University of Waterloo, Waterloo, Canada

Abstract— **Hematopoietic Stem Cells (HSCs) form blood and immune cells and are responsible for the constant renewal of blood. To produce new blood cells, HSCs proliferate and differentiate to different blood cell types continuously during their lifetime. Hence they are of substantial interest in stem cell therapy and cancer research. To classify HSCs to different groups, they must be observed/tracked over time and their key features including cell size, shape, and motility must be extracted. The manual tracking is an onerous task and automated methods are in high demand.**

The first stage of an semi-automatic/automatic tracking system is cell segmentation. In our previous work we addressed the cell segmentation/localization problem. Modelling adjacent or splitting cells is very challenging and our previous methods might fail to accurately model a group of adjacent cells or a splitting cell. In this paper we address this issue and propose a deconvolution method to precisely model individual HSCs as well as adjacent (splitting) HSCs. An optimization algorithm is combined with a template matching method to segment cell regions and locate the cell centers.

I. INTRODUCTION

Advanced techniques in digital image processing and pattern recognition must be applied to a huge number of bio-cellular images in semi-automated/automated digital cytometry systems to improve our understanding of cellular and inter-cellular events and to achieve significant progress and new discoveries in biological and medical research.

Microscopic cell image segmentation as an object segmentation problem remains an attractive and challenging task due to the often corrupted or blurred images, high noise, the presence of clutters, and the difficulties of adapting and extending available image segmentation approaches to the applications of cell imaging [1], [2], [3], [4]. A variety of semi-automatic or automatic methods including thresholding, watershed, nearest neighborhood graphs, the mean shift procedure and deformable models have been proposed for cell segmentation. Geusebroek et al [5] introduced a method based on Nearest Neighbor Graphs to segment the cell clusters. Meas-Yedid et al [6] proposed a method to quantify the deformation of cells using snakes. Kittler [7], Otsu [8] and Wu [9] have used thresholding methods. The mean shift procedure method was proposed by Comaniciu et al [2] for cell image segmentation for diagnostic pathology. Watershed has been used by Markiewicz et al [10] for segmentation of bone marrow cells.

This research has been funded by the Natural Science and Engineering Research Council of Canada (NSERC).

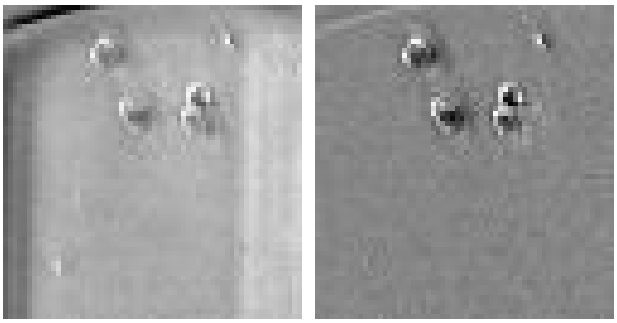

Fig. 1. Left: Original HSC image. Right: After background estimation/subtraction.

In this paper, a novel deconvolution method in the form of an optimized ellipse fitting algorithm is proposed to locate the individual Hematopoietic Stem Cells (HSCs). The proposed method has been successfully applied for modelling HSCs and identifying their locations in phase contrast microscopic images.

To produce the data for this study, HSC samples are first extracted from mouse bone marrow and cultured in custom arrays having up to forty wells. HSCs are then imaged using manual focusing through a 5X phase contrast objective using a digital camera (Sony XCD-900). Images were sampled every three minutes over the course of several days. A small fraction of a typical HSC microscopic image is depicted in Fig. 1.

II. THE PROPOSED METHOD

In our previous work [11] we characterized a typical HSC in a microscopic image as an approximately circular object with a darker interior and a bright boundary. The proposed cell model works well to localize a specific HSC phenotype, however the performance of the algorithm drops if there are significant illumination variations during phase contrast imaging. Moreover it is developed for a specific HSC phenotype and performs poorly for the phenotypes that do not maintain a uniform bright boundary and dark interior. In [12] we introduced a more general model which is robust against noise and can be applied to the different HSC phenotypes.

Although our previous methods [11], [12] perform well to locate non-dividing and dividing cells, they are not capable of accurately model splitting or close by cells. As a result

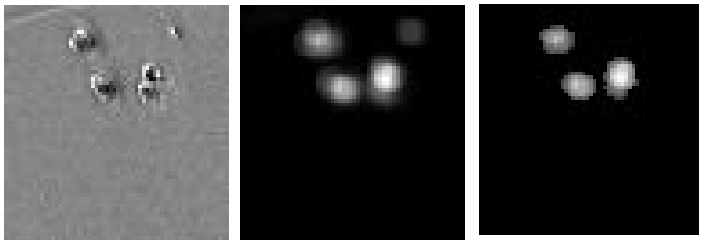

(a) (b) (c)

Fig. 2. (a) Original HSC image after background subtraction. (b) Elliptical mean square of (a). (c) Binary image of (b) showing cell regions.

they might fail to precisely locate the adjacent cells and in turn are prone to generate erroneous results in such cases.

To address this issue, assume that in advance we have segmented the cell areas containing individual or groups of cells. Then locating the cell centres or cell centroid (depends on the cell shape parameters) is essentially an inverse problem which can be addressed in the form of a deconvolution problem such that a set of cell(s) shape parameters must be found for optimal representation of cell(s) segmented area. The proposed method solves the inverse problem using an optimized ellipse fitting method to find the optimal cell(s) parameter set and locate the cell centres. This is a generic method, capable of modelling different cell types with changes in the model parameters, and robust against illumination variations. Our proposed method consists of background subtraction, cell template generation, template matching, and optimized ellipse fitting.

III. Background Estimation

We have employed the same method for background estimation and subtraction as in our previous work [12]. In this method we assume F and I are pure and corrupted sequences, respectively, of $N \times M$ images. F is corrupted by spatial illumination variations v over time and temporal additive noise n in each frame. We also assume that v and n are identically distributed, independent from each other and both independent from I

$$I = F + e \tag{1}$$

where $e = v + n$. Each pixel I_{ijt} represents a pixel in 3 spatio-temporal dimensions such that

$$I_{ijt} = F_{ijt} + e_{ijt} \tag{2}$$

where

$$e_{ijt} = v_{Spatial}^{\{[1:T]\}} + n_{Temporal}^{\{[1:N][1:M]\}} = v_{ij}^{\{[1:T]\}} + n_{t}^{\{[1:N][1:M]\}} \tag{3}$$

Then the pure signal F is estimated by

$$\hat{F} = I - \hat{e} \tag{4}$$

where for each spatio-temporal pixel F_{ijt} we have $\hat{F}_{ijt} = I_{ijt} - \hat{e}_{ijt}$.

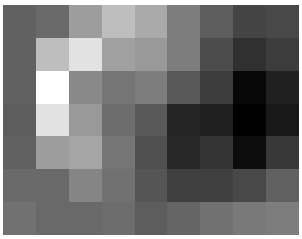

Fig. 3. Sample cell template.

IV. Elliptical Mean Square Model

HSC can be observed by a set of pixels with significant intensity variations against the uniform background in the background corrected image. Hence we model HSCs as elliptical anomaly to segment the cell regions assuming (c_x, c_y) as center coordinates, a and b as horizontal and vertical radii of the cell. The continuous elliptical cell is spatially discretized as

$$\frac{(x_l - c_x)^2}{a} + \frac{(y_l - c_y)^2}{b} \leq 1, \tag{5}$$

where (x_l, y_l) are coordinates of cell pixels. So the set of inside cell pixels can be explained by

$$C_p(c_x, c_y, a, b, I) = \{I_{ij} | \ \frac{(c_x - i)^2}{a} + \frac{(c_y - j)^2}{b} \leq 1 \ \}, \tag{6}$$

from which we compute the sample mean of square-intensities of cell pixels

$$\bar{C_p} = \frac{\sum_l {C_p^l}^2}{|C_p|} \tag{7}$$

To discriminate cells from background, the resultant mean square image is classified to cell and background by minimizing the inter-class variance as can be observed in Fig. 2(b).

V. Cell Template Generation

In contrast with our proposed mathematical cell template in [11] that was introduced based on attributes of a specific HSC phenotype such as uniform bright boundary and dark inside, here using user interactions a more general cell template applicable to different cell types will be generated. In this way user selects some cells in a few frames of the video clip by clicking on the upper-left and lower-right corners of a rectangular box that the cell is surrounded in. The selected cells are averaged to generate the cell template:

$$C_{tpl} = \frac{1}{N_c} \sum_{n=1}^{N_c} C_{rect}^n \tag{8}$$

where C_{tpl} and C_{rect}^n are 2-Dimensional matrices. Then the cell template is convolved with the background corrected video clip to generate a correlation map. Cell template and the correlation map obtained by applying the cell template are depicted in Fig. 3 and 4(a) respectively. The brighter pixels in the correlation map show the highly correlated

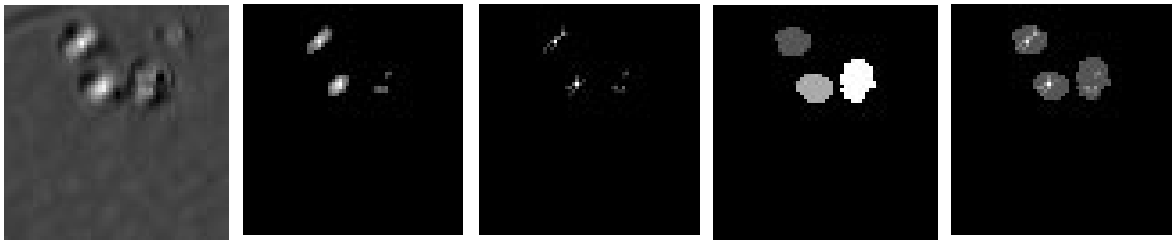

(a) (b) (c) (d) (e)

Fig. 4. (a) Correlation map obtained by applying the cell template to the background corrected image. (b) Thresholded correlation map. (c) All 1-D local maxima with distance 1-pixel located in each row and each column of (b). (d) Labelling the cell segmented regions. (e) Superimposing (c) on (d).

points which are more likely to be a cell centre. To remove the unlikely cell centre candidates the correlation map is thresholded as depicted in Fig. 4(b).

VI. Ellipse Fitting

So far we have segmented the cell regions using classification of elliptical mean square map to cell and background regions, and located the cell centre candidates by applying the cell template and thresholding the correlation map. The set of cell parameters in a typical video frame is explained by f:

$$f = \{(c_x, c_y, a, b, \theta)|\ (c_x, c_y) \in C_{cnt}\} \tag{9}$$

where (c_x, c_y) are cell centre coordinates which will be extracted from the set of cell centre candidates C_{cnt}. Radii of elliptical cell are represented by (a, b) and θ is orientation of the cell. To locate the cell centres, we propose the following *Maximum A Posteriori* (MAP) problem to be solved:

$$\hat{f} = arg\ \left\{ \underset{f}{max}\ \ P(f|\ I) \right\} \tag{10}$$

HSCs in our problem have a quasi-circular shape and without losing the generality we can assume $\theta = 0$ so that (9) can be simplified to:

$$f_\theta = \{(c_x, c_y, a, b)|\ (c_x, c_y) \in C_{cnt}\} \tag{11}$$

and as a result (10) can be rewritten as

$$\hat{f}_\theta = arg\ \left\{ \underset{f_\theta}{max}\ \ P(f_\theta|\ I) \right\} \tag{12}$$

To solve the MAP problem (12) and find the cell centres and ellipse's radii for each cell, we apply an optimized search method by fitting elliptical shapes to the segmented cell regions and searching for the maximum of $R(\alpha, \beta, \delta)$ defined as

$$R(\alpha, \beta, \gamma) = \frac{\alpha}{\beta + \gamma} \tag{13}$$

where α is covered area of the segmented region by ellipse (or ellipses), β is the area of the segmented cell region that is not covered by any ellipse, and γ is the area outside of the segmented cell region that is covered by an ellipse (or ellipses). Maximum of (13) must be found over the search space which consists of cell centre candidates C_{cnt} and cell radii candidates C_{radi}. The former is obtained by locating all 1-Dimensional local maxima with distance one pixel in each row and each column of thresholded correlation map as it is depicted in Fig. 4(c). The latter is a $2 \times N_r$ matrix which is set empirically by observing HSC over different video clips, where N_r is the number of radii pairs.

VII. Results

To derive the results, first the estimated background is subtracted from the original video clip to eliminate the noise and illumination variations and to obtain a video clip with uniform background as depicted in Fig. 1. The proposed elliptical mean square is then applied to the background corrected image (Fig. 2(a)) as can be seen in Fig. 2(b). In the next step the mean square image is classified to the cell regions and the background as it can be observed in Fig. 2(c). Fig. 3 shows the generated cell template while the correlation map, thresholded correlation map, and located 1-D local maxima with 1-pixel distance are depicted in Fig. 4(a), (b), and (c) respectively. Fig. 4(d) shows the labelled segmented regions. The superimposed 1-D local maxima on segmented cell regions is depicted in Fig. 4(e). Fig 5(a) shows the first segmented cell region with superimposed cell centre candidates for this region. A typical hypothesis $f_h^{Rig_1}$ is showed in Fig 5(b) in which we can observe two elliptical cells are fitted in the segmented region. Optimal hypothesis $f_{best}^{Rig_1}$ which maximizes R for this region is depicted in Fig. 5(c). As we can observe an elliptical cell almost perfectly covers this region. White and light gray represent α, dark gray represents β while γ is represented by black in Fig. 5. Fig. 5(c), (d), and (e) respectively show the segmented region of a splitting cell with superimposed cell centre candidates, a typical hypothesis $f_h^{Rig_3}$, and optimal hypothesis $f_{best}^{Rig_3}$ for this region which maximizes R by fitting two elliptical cells.

The proposed method is applied to different HSC video clips and generated promising results. As can be observed in Fig. 6, the proposed optimized elliptical cell fitting method is able to identify both non-dividing and the more challenging dividing cells so that the cell centres are almost precisely located for each case.

VIII. Conclusions and Discussions

Modelling and locating groups of adjacent or splitting cells is a very difficult and challenging task. Most of the present cell segmentation methods are not capable of accurately model splitting or close by cells and fail to precisely locate them.

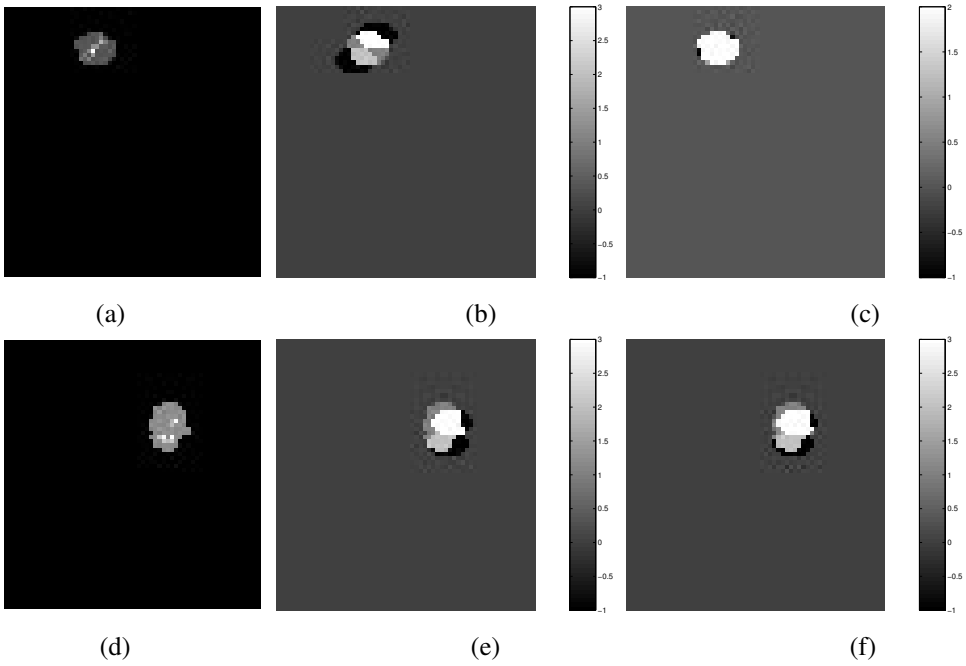

Fig. 5. Left column: Segmented region with superimposed cell centre candidates. Middle column: A typical hypothesis $f_h^{Rig_k}$, fitting two elliptical cells in the segmented cell region. Right column: Optimal hypothesis $f_{best}^{Rig_k}$ which maximizes R for region k; (a),(b) and (c) represent region one ($k = 1$). (d),(e) and (f) represent region three ($k = 3$).

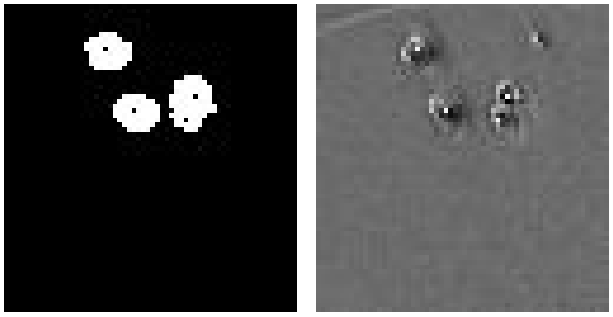

Fig. 6. Located cell centres; Left: Superimposed in segmented HSC image. Right: Superimposed in background corrected HSC image.

In this paper we addressed this issue as an inverse problem represented in the form of a deconvolution problem. Our proposed method solves the deconvolution problem by searching the optimal shape parameters (for each individual cell) using an optimized ellipse fitting method to represent the segmented area. This is a generic method, capable of modelling different cell types by designing the proper shape model. The optimized cell shape parameters can be then extracted using the same search method as the proposed method by optimizing the cost function that fits the cells in the segmented area.

Moreover our method is robust against illumination variations. The spatio-temporal background subtraction in the proposed method removes the temporal noise caused by illumination variations and spatial noise caused by CCD camera non-uniformities.

REFERENCES

[1] D. Comaniciu, D. Foran, and P. Meer, "Shape-based image indexing and retrieval for diagnostic pathology," in *International Conference on Pattern Recognition*, 1998, pp. 902–904.

[2] D. Comaniciu and P. Meer, "Cell image segmentation for diagnostic pathology," *Advanced algorithmic approaches to medical image segmentation: State-of-the-art applications in cardiology, neurology, mammography and pathology*, pp. 541–558, 2002.

[3] E. Campo and E. Jaffe E, "Mantle cell lymphoma," *Arch. Pathology Lab. Med.*, vol. 120, no. 1, pp. 12–14, 1996.

[4] I. Bauman, R. Nenninger, H. Harms, H. Zwierzina, K.Wilms, A.C. Feller, V.T. Meulen, and H.K. Muller-Hermelink, "Image analysis detects lineage-specific morphologic markers in leukemia blast cells," *American Journal of Clinical Pathology*, vol. 105, no. 1, pp. 23–30, 1995.

[5] J.M. Geusebroek, A.W.M. Smeulders, and F. Cornelissen, "Segmentation of cell clusters by nearest neighbour graphs," in *Proceedings of the third annual conference of the Advanced School for Computing and Imaging*, 1997, pp. 248–252.

[6] V. Meas-Yedid, F. Cloppet, A. Roumier, A. Alcover, J-C Olivo-Marin, and G. Stamon, "Quantitative microscopic image analysis by active contours," in *Vision Interface Annual Conference 2001 - Medical Applications*, 2001.

[7] J. Kittler and J. Illingworth, "Minimum error thresholding," *Pattern Recognition*, vol. 19, no. 1, pp. 41–47, 1986.

[8] N. Otsu, "A threshold selection method from gray-level histograms," *IEEE Transactions on Systems, Man, and Cybernetics*, vol. 9, no. 1, pp. 62–66, 1979.

[9] K. Wu, D. Gauthier, and M. Levine, "Live cell image segmentation," *IEEE Transactions on Biomedical Engineering*, vol. 42, no. 1, pp. 1–12, 1995.

[10] T. Markiewicz, S. Osowski, L. Moszczyski, and R. Satat1, "Myelogenous leukemia cell image preprocessing for feature generation," in *5th International Workshop on Computational Methods in Electrical Engineering*, 2003, pp. 70–73.

[11] N. N. Kachouie, P. Fieguth, J. Ramunas, and E. Jervis, "Probabilistic model-based cell tracking," *International Journal of Biomedical Imaging*, vol. 2006, pp. 1–10, 2006.

[12] N. N. Kachouie and P. Fieguth, "A statistical thresholding method for cell tracking," in *IEEE International Symposium on Signal Processing and Information Technology*, 2006, pp. 222–227.